Chapter 8
Lung Imaging in Animal Models

Emma Lefrançais, Beñat Mallavia and Mark R. Looney

Introduction

Animal models of lung injury and repair are designed to study inflammatory cell migration, cell signaling, and disruptions of the alveolar-capillary barrier. In vitro and ex vivo experiments, described in other chapters, have led to significant advances, but may involve the isolation and manipulation of cells that can affect their function. Cultured lung cells undergo phenotypic transformation, and terminal assays like histologic preparations, bronchoalveolar lavage, or cell sorting methods only provide a single snapshot in the evolution of the injury model. Even if the assays are useful in understanding what cells are present in the tissue and to quantify different parameters of lung injury, some important features like spatial and dynamic interactions can only be understood from live imaging. Lung imaging integrates the four dimensions of the tissue, one of time and three of space. Indeed, time is necessary to determine which physiologic processes are in progress or to estimate their rate. Lung imaging enables monitoring of the lung in its native setting and in real-time throughout the course of disease.

Lung Imaging Background

Lung Imaging Challenges and Peculiarities

Tissue microscopy has gained increased attention since the important advances in optical imaging technology. However, these methods were first applied to more

E. Lefrançais · B. Mallavia · M.R. Looney (✉)
Department of Medicine, University of California, San Francisco, San Francisco, CA, USA
e-mail: mark.looney@ucsf.edu

L.M. Schnapp and C. Feghali-Bostwick (eds.), *Acute Lung Injury and Repair*,
Respiratory Medicine, DOI 10.1007/978-3-319-46527-2_8

accessible tissues, like the skin, cremaster muscle, or lymph nodes. The lung is probably one of the most difficult organs to observe under physiologic conditions as immobilization and exposure to the atmosphere interfere with its normal function. Indeed, imaging lung in vivo must overcome major obstacles. First, access to the organ requires opening of the chest wall, which leads to lung deflation without the intervention of positive pressure ventilation. Second, the motion due to both respiration and cardiac contractions further complicate the goal of a stable lung preparation. Next, the air-filled alveolar spaces pose an optical challenge, since air has a different refractive index than tissue. Lastly, the lung has a unique and delicate structure highly susceptible to mechanical and pro-inflammatory stress. These obstacles have been surmounted by different means including microscopic advancements, novel lung stabilization methods or the improvement of noninvasive imaging techniques. The lung is not only distinctive in its difficulty to image but also in its physiology. Indeed, the lung is the largest epithelial surface of the body in contact with the environment, the alveolar surface of the human lung being the size of a tennis court. Made for gas exchange, this area is also the site where potential pathogens meet one of the first lines of defense. Pulmonary circulation is peculiar as well, made of numerous interconnected capillary segments. These capillaries are particularly small, varying from 2 to 15 mm in diameter, which make the circulation of larger blood cells potentially difficult. Leukocyte sequestration and emigration mechanisms are consequently different from the systemic circulation. All these factors make lung imaging challenging and yet very promising to acquire unique knowledge.

History of Lung Imaging

The first microscopic observation of the lung was made in 1661 in Italy by Marcello Malpighi [1]. He was one of the first scientists to use the recently invented compound microscope, with an objective and an eyepiece lens. After failures using mammalian models, he used the frog and was the first person to observe and describe the lung capillaries and alveoli. His description completely changed perceptions of the structure of the lung that was thought to be similar to kidney or liver. He introduced for the first time the notion of vessels attached to an infinite number of air cavities. Two hundred fifty years later, Hall presented in 1925 a method for intravital microscopy of the lung in cats and rabbits [2]. To minimize respiratory movement he exteriorized a lobe out of the chest and fixed it with small clamps. However, exteriorization and fixation significantly alters the physiology of the lung and its circulation. To facilitate visual access to the lung in vivo, scientists then developed a series of increasingly refined thoracic window preparations. The first window was developed in the cat by Wearn et al. [3]. A window was excised in the thorax and the lung was transilluminated by creating a second window in the diaphragm through which the light beam of an arc lamp was passed. Curare was used to abolish respiratory movement and ventilation was maintained compressing

the chest at short intervals. In 1939, Terry et al. [4, 5] constructed a thoracic window consisting of a metal cylinder mounted with a cover glass. Using cats, he inserted it in between two ribs and attached the microscope to the thoracic wall to follow respiration movement. To remove the air that entered the pleural cavity during surgery, he used an exhaust tube, allowing the lung to adhere to the cover glass. This window preparation permitted the observation of lung under closed thoracic conditions. Later, 1963, De Alva and Rainer [6] and Krahl [7] installed an intercostal window prosthesis in rabbit and dog that allowed observation of spontaneously breathing animals for several months. Mechanical ventilation was used during and after the surgery until spontaneous breathing was reestablished, removing air with a syringe. To manage the respiration movement, the microscope was focused at end-expiration or peak inspiration, which provided enough stabilization to acquire images. The thoracic window was improved by Wagner et al. [8] in **dogs** with a more elaborate suction system that was used to arrest cardiorespiratory movements allowing stable imaging of the live lung. The dogs were ventilated during the observation period.

Fluorescence-Based Imaging Techniques

Since the invention of the two lens microscope in the beginning of the seventieth century, advances in microscope technology have been considerable, improving image resolution, depth of imaging and sensitivity. Fluorescence microscopy is the technique that provides the highest spatial resolution among the available imaging techniques. We will describe briefly the microscopic techniques that enable live imaging and that can be used for lung imaging.

Microscopy Techniques Currently Used for Fluorescence Imaging

Imaging of a live tissue demands sufficient excitation energy to access to deep tissue layers but without creating photo damage. From conventional wide-field microscopy, to confocal and two-photon microscopy, the development of novel microscopy techniques has attempted to improve resolution (how much detail a user can observe, defined as the shortest distance between two points that a user can still see as separate images) and sensitivity (the ratio between signal to noise).

- ***Wide-field microscopy***

In wide-field microscopy, the entire sample is excited with a specific band of wavelengths that matches the excitation of the fluorophore. The emitted signal is separated from the excitation light by specific filters. In this technique, fluorophore

excitation is not restricted to the plane of focus, which causes image blur. It is therefore problematic to image structures deep below the surface or if stained structures are stacked on top of each other.

- ***Confocal microscopy***

In confocal microscopy, the sample is excited by a laser which is focused to a single spot. Then, only the emitted signal from the focal plane is detected due to passage through a pinhole (Fig. 8.1a). Elimination of out of focus background leads to excellent spatial resolution and enables acquisition of images from within thick samples. Three-dimensional reconstructions can be produced when different illuminated planes are combined. However, during live imaging, a major drawback of confocal microscopy is that a large proportion of emitted light is discarded, blocked

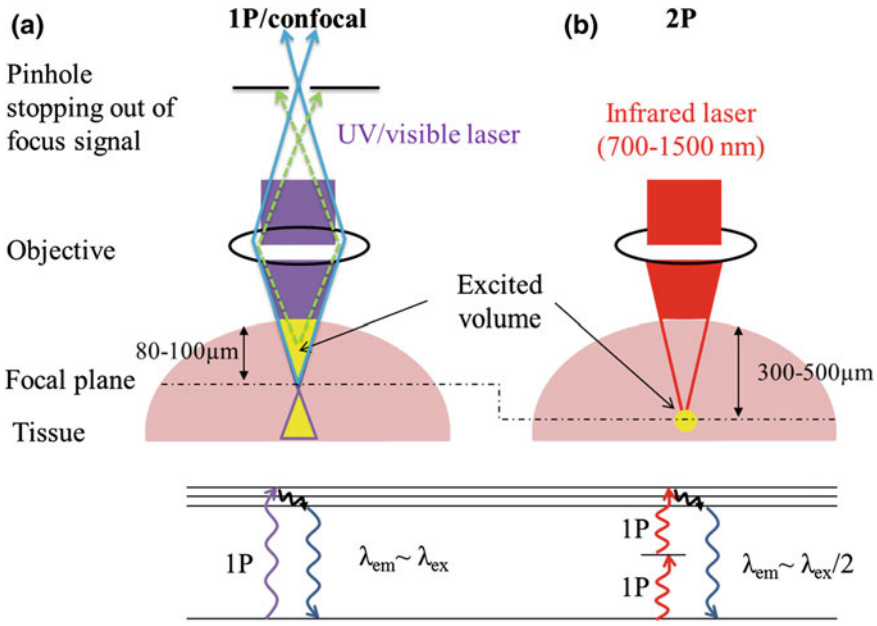

Fig. 8.1 Fluorescence microscopy imaging techniques used for intravital microscopy. **a** Confocal microscopy. (*Top*) In confocal microscopy, excitation and emission occur in a relative large volume around the focal plane (*yellow triangles*). The off-focus emissions are eliminated through a pinhole. (*Bottom*) In 1P microscopy, a fluorophore absorbs a single photon with a wavelength in the UV–visible range of the spectrum (*purple arrow*). After a vibrational relaxation (*black arrow*), a photon with a slightly shorter wavelength is emitted (*blue arrow*). Confocal microscopy enables imaging at a maximal depth to 80–100 µm. **b** Two-photon microscopy. (*Top*) Emission and excitation occur only at the focal plane in a restricted volume (*yellow spot*), and for this reason a pinhole is not required. (*Bottom*) In this process a fluorophore absorbs almost simultaneously two photons that have half of the energy (twice the wavelength) (*red arrow*) required for its excitation with a single photon. Two-photon excitations typically require IR light (from 700 to 1500 nm). Two-photon microscopy enables imaging at a maximal depth of 300–500 µm

by the pinhole. To establish sufficient sensitivity requires a strong excitation signal, which can cause photo damage and dye bleaching.

- ***Two-photon microscopy***

The photo damage and bleaching that limit confocal microscopy can be overcome using two-photon (2P) microscopy. 2P excitation occurs when two lower energy photons (together having the equivalent energy of a single higher energy photon) are absorbed by a fluorophore. The probability of nearly simultaneous absorption of two photons is very low and will occur only at the focus of a high-energy pulsed laser (Fig. 8.2b). 2P is superior to confocal microscopy in the imaging of live tissues for two major reasons. First, only the point of focus is excited, inducing less photo damage and increasing the sensitivity. Second, the infrared excitation light used in 2P is less prone to scattering and penetrates deeper in living tissue, up to several hundred microns deep (compared with <80 μm with confocal). This makes it a very powerful technology for lung in vivo imaging.

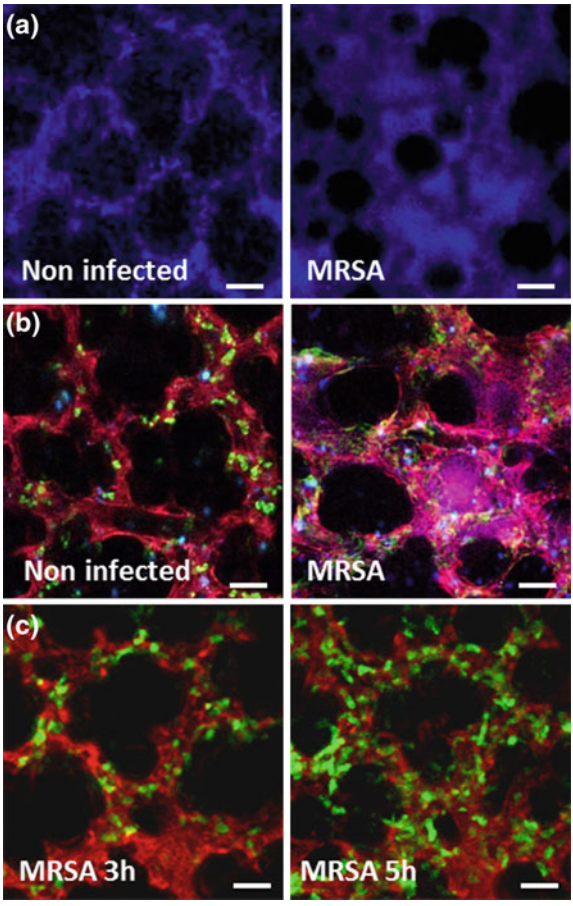

Fig. 8.2 Examples of fluorescence intravital microscopy applications to study lung injury. Characteristics of acute lung injury are observed after intratracheal instillation with MRSA (Methicillin-resistant *Staphylococcus aureus* -5×10^7 cfu). **a** Vascular permeability, observed by leakage into the alveolar space of i.v. Cascade Blue dextran. **b** Neutrophil elastase activity is monitored by the cleavage of a far red fluorescent substrate (NE680 FAST, Perkin Elmer), shown in pink in MRP8-Cre × mTmG lungs (GFP: neutrophils, tdTomato: ubiquitous). **c** Neutrophil recruitment is observed during the course of infection in MRP8-Cre × mTmG lungs at 3 and 5 h after infection. *White bars* indicate 30 μm

Lung Fluorescence Imaging Preparations

Technological advances in microscopy allow the acquisition of high-resolution images of the subpleural layers of the lung to analyze cellular and subcellular processes. Lung fluorescence imaging preparations can take three main forms: explanted tissues, live lungs slices placed under the flow of suitable medium, and intravital imaging where the lung is maintained in its natural microenvironment.

Live Lung Slices (LLS)

Description of LLS Preparation

The live lung slice method consists of partitioning the lung in thick slices, which are then carefully maintained to assure tissue viability. To do so, after the exsanguination of the animal, a cannula is placed intratracheally and lungs are inflated with 1.5–2 % liquid low melting agarose to maintain lung structure. The lungs are extracted and agarose is solidified in cold physiological medium. With the use of a micro-slicer or a vibratome, 150–300 μm thick serial slices are obtained. The vibration offers the possibility of cutting living tissue with a minimal injury. The slices are maintained in cell culture media at 37 °C and 5 % CO_2. Lung slices are normally used in the first 8 h although they have been used up to 2–3 days after sampling [9]. The lung slices have normal cell activity allowing the study of cell interactions and at the same time the structure of the alveoli is maintained to allow the 3D imaging of cell movements. For complete tissue preparation methods review, please see Thornton et al. [10].

Advantages and Disadvantages of LLS

LLS preparations have several advantages in comparison to fixed tissue imaging. First, fixed tissue samples are usually much thinner than live lung slices. The increased thickness of the live slices allows the study of three-dimensional cell movements that would be lost in thinner preparations or cellular monolayers. Second, and more importantly, unlike the static fixed images, LLS allow the study of time-dependent processes ranging from fast cell–cell interactions to the study of complex and slow pathogenic immune responses in the lung. Third, the LLS technique is a useful tool to study cellular interactions deep in the lung where intravital imaging or the isolated, perfused lung preparation cannot reach due to the excessive thickness. Because only a section of lung is studied with LLS preparations, it has important limitations such as the loss of blood and lymph circulation and the lack of neural input. These considerations are very important in studies requiring cell egress from other organs or other parts of the lung. Leukocyte activation induced by the isolation procedure may also be a concern.

Application of LLS in Lung Injury Studies

- ***Cell death analysis***

In a work aimed to establish LLS as a suitable ex vivo technique to investigate the immunomodulatory effects and the characterization of cytokine production after LPS and other challenges, cell death was imaged by live/death fluorescence using confocal microscopy [9]. To distinguish living from dead cells, different dyes are used, such as Acridine Orange and Propidium Iodide. These markers allowed a better characterization of rat type II pneumocytes in an in situ patch clamp study [11]. TUNEL fluorescence analysis is also a very useful staining approach to study cell death. Jacobs et al. used this technique to study ROS-induced cell apoptosis [12].

- ***Ca^{2+} measurement***

Pulmonary neuroephithelial bodies (NEB) are organized as clusters of pulmonary neuroendocrine cells during the development of the lung, and 4-Di-2-ASP fluorescent staining can be used to identify them in sliced lung preparations. Ca^{2+} signaling in the NEB microenvironment has been the focus of several studies. To facilitate imaging, Ca^{2+}-specific fluorescent dyes have been developed, from the commonly used Fluo-3 to its brighter analog Fluo-4. The use of these dyes allows real-time imaging of cellular Ca^{2+} flux using confocal microscopy [13, 14].

- ***Tissue/cell identification***

The use of fluorescent antibodies in LLS preparations has improved protein and cellular identification due to the greater antigen accessibility compared with whole lung approaches. The use of Surfactant A and alveolar type II cell-specific antibodies allowed the identification of alveolar type II cells and the lamellar bodies contained within the cells [15].

- ***Transgenic mouse studies***

The introduction of fluorescent markers opened the possibility to easily track and image target cell types or even cell subpopulations. Using a transgenic mouse where a yellow fluorescent protein expression is under the control of a promoter specific to antigen-presenting cells (CD11c-EYFP), Major Histocompatibility Complex (MHC) class II expression was studied. The lung slices were incubated with LPS and other pro-and anti-inflammatory molecules and the confocal fluorescence images showed that MHC-II expression was increased with pro-inflammatory challenges and repressed with dexamethasone [9].

Isolated, Perfused Lung Method (IPL)

Description of the IPL Method

In the isolated, perfused lung preparation, the left pulmonary artery is cannulated and perfused with autologous blood or a physiologic salt solution allowing passive

drainage through the left ventricle. The lungs are ventilated with normal air or humidified gas containing different concentrations of oxygen and positive end-expiratory pressure is maintained. Using a perfusion pump, experimental agents can be added to the perfusate and introduced in the lung circulation. The lungs are suspended from a force displacement transducer to measure lung weight changes, while the whole system is maintained in a closed chamber with controlled humidity and temperature.

Advantages and Disadvantages of IPL

The main advantage of IPL technique over the live intravital approach is the unmatched stability of the sample. This important feature has permitted the use of directed microinjections of fluorescent dyes into endothelial or epithelial cell layers in the lungs [16]. Perfused whole lung preparations are a better approach to study lung physiology than LLS preparations. IPL preparations do not have the injured cut surfaces at the top and bottom of the preparation, which may induce undesirable effects when studying organ functionality. Vascular leakage is also better studied in isolated lungs than in LLS [17]. A clear disadvantage of isolated lung preparations is that it lacks the effects of the normal (or induced) physiological changes that occur systemically. This effect diminishes the possibility of leukocyte chemoattraction to the lungs from the bone marrow and circulation, which is an important limitation in inflammation-related studies. A possible leukocyte activation effect induced by the pump-assisted circulation used in the preparation of IPL is another disadvantage when compared with lung intravital microscopy [18].

Application of IPL to Lung Injury Models

- ***Tissue/cell identification***

The labeling of mitochondria with fluorescent tags has allowed for the study of mitochondria transference in lung injury models. Islam et al. showed that mouse bone marrow-derived stromal cells, containing red fluorescent mitochondria, were located adjacent to epithelial cells minutes after their instillation into LPS-challenged isolated perfused lungs. In a further experiment, they showed by confocal microscopy that the fluorescent mitochondria were transferred to alveolar type II cells in a gap junction dependent process [19]. The use of other mitochondria markers (Mitotracker green, Ca^{2+} binding Rhod 2AM) allows their identification in endothelial cells [20].

- ***Leukocyte trafficking***

Leukocytes are critical mediators of lung injury induced by endotoxemia, and the time that leukocytes spend in lung microvessels (venules and capillaries) depends on their activation state as well as the activation state of the endothelium. The use of

fluorescence microscopy and R6G-rhodamine revealed that LPS-challenged microvessels retained leukocytes for a longer time than unchallenged lungs. The passage time is easily quantified in the surface vessels of isolated and perfused lungs without introducing any mechanical injury to the lungs [21].

- ***ROS production***

Reactive oxygen species (ROS) production can be measured using fluorescence microscopy and the 2′–7′-dichlorodihydrofluoroscein acetate dye [20]. This technique was employed by Ichimura et al. to show that physical pressure-induced stress is able to promote ROS-triggered endothelial cell expression of P-selectin.

- ***NO production***

Nitric oxide (NO) is a potent controller of the vascular tone in systemic and pulmonary vessels. Shear stress can promote the production of NO in endothelial cells. In 2000, in situ fluorescence procedures using IPL showed that shear stress was able to induce endothelial cell NO using a NO probe (diaminofluorescein diacetate), which was preceded by intracellular changes in Ca^{2+} detected using a fluorescent probe (Fluo-3) [22].

Lung Intravital Microscopy Methods (IVM)

Description of the Lung IVM Method

To observe the lung in a more physiological manner, it should be imaged in vivo. As discussed earlier, challenges faced with lung imaging compared to other organs are its intrinsic motion and the maintenance of breathing after opening the thorax. Different approaches have been developed to address these issues including (a) maintaining mechanical ventilation or reestablishment of spontaneous breathing, (b) the structure and composition of the window in contact with the lung, and (c) the management of cardiorespiratory motion.

- ***Ventilation and closed thorax imaging***

Access to the lung requires opening of the thorax, which will cause lung collapse in the absence of positive pressure ventilation. Therefore, most of the preparations will use mechanical ventilation. Animals are anesthetized and tracheally intubated to be ventilated with room air or enriched oxygen. The animal is placed on a warming pad set to 37 °C to help maintain body temperature. To prevent dehydration, physiologic crystalloid solutions should be administered every hour or continuously. In some experiments, the thorax is closed after placing the window. To recover spontaneous breathing, the removal of the air introduced in the pleural cavity is required by vacuum or syringe suction. Mechanical ventilation is maintained until the lung is able to re-expand. Fingar et al. used a thoracic window implanted in rats to follow for 2 weeks the progression of pulmonary edema and

alveolar flooding after lung injury by monitoring the leakage of vascular dyes [23]. Thoracic windows have been maintained in dog and rabbits for several months [6, 7]. Implanting a window has the advantage of not interfering with physiological respiration. However, because the motion is not controlled, it is not suited to high-resolution acquisition.

- ***Thoracic windows specificities***

Once the thorax is open, it is important for high-resolution images to have stable windows with good optical properties and minimal interference with the normal structure and function of the lung. Most of the thoracic windows have used a metallic structure, first described by Terry et al. [4], to be introduced in between two adjacent ribs. The air from the pleural cavity is removed by suction or a syringe to bring the lung close to the observation window, which can be a cover glass [4, 24] or a transparent membrane made of Cronar [6] or Teflon [25]. To prevent the lung from dehydrating or cooling, the Teflon membrane used by Kuhnle et al. is covered by a warmed and bubbled Tyrode's solution. Metal and glass windows are efficient but their rigidity can induce trauma upon the delicate lung surface. Other approaches use less invasive methods, particularly in the mouse. Tabuchi et al. [26] used a polyvinylidene membrane sealed with glue over the ribs, and Kreisel et al. [27] attached the lung tissue to the bottom of a coverglass with tissue adhesive (VetBond). However, irritation may be produced from the moving lung touching the membrane potentially invoking an inflammatory response.

- ***Control of lung motion***

One of the first approaches used on cats [3] and rats [23] was to use paralyzing agents to halt respiration. Another way to increase the time of stabilization is to temporarily suspend the respiration for 30 s [28] or in one of the two lungs by clamping the bronchus while ventilating the other lobe [29]. However, in these techniques where the respiration is blocked, the observed tissue will suffer from impaired oxygenation, which will undoubtedly affect the observed physiology. Without interrupting respiration, another technique has been to image the lung once every respiratory cycle, when the lung stops moving for a moment and comes back to the previous cycle position, at the end of the expiratory phase. This approach has been applied by Kuhnle et al. [25] and Tabuchi et al. [26]. This timing can be achieved by matching the ventilation rate and the acquisition. Indeed, imaging every 0.5 s with a ventilator rate of 120 breaths/min by Kreisel et al. [27] enables image acquisition once every breath cycle. More recently, in an effort to obtain more physiologic imaging, Fiole et al. did not use any stabilization procedure in the mouse lung during imaging, but instead corrected the images post hoc [30]. Every minute, a series of images was acquired and just one image was retained without any deformation. Lung structure was used as a frame of reference to select the correlated images by computer analysis.

Wagner et al. [8] addressed in an efficient way the obstacle of cardiorespiratory movement in live animal imaging using a thoracic window with built-in suction,

providing enough stabilization for real-time microscopy. A similar technique, adapted from Wagner's thoracic window coupling suction to gently immobilize the lung on a glass coverslip has been recently adopted and miniaturized for mice by Looney et al. [24]. Different mouse windows were developed by groups in Germany [26], Japan [29] and USA [24, 27, 31]. The application of these lung intravital microscopy methods to mice has allowed access to the tools available with transgenic animals.

Advantages and Disadvantages of Intravital Microscopy

- ***Advantages***

One advantage of fluorescence intravital microscopy is the high-resolution enabled by all fluorescent techniques. Compared to other techniques described for fluorescent imaging, lung intravital imaging makes it possible to observe lung injury under physiological conditions and with maintenance of the lung microenvironment. The preservation of blood and lymphatic circulation is one the main attractive features of IVM, which is important to study vascular permeability and leukocyte recruitment. It is consequently one of the most powerful approaches to study processes in lung injury animal models at a cellular and molecular scale.

- ***Disadvantages***

One of the major limitations of intravital microscopy is the restricted ability to image deep in tissues. Imaging with two-photon excitation is confined mainly to 30–100 μm below the pleural surface, accessing only the most superficial layer of the lung. It may be a concern if the injury and inflammation in this superficial layer differ from the rest of the tissue. Moreover, the surgical preparation needed to access the lung could induce trauma that could have deleterious effects upon the microcirculation. Studies must be evaluated carefully considering the influences that may alter the normal physiology of the lung. Lastly, even though these IVM methods enable the acquisition of lung images up to several hours, it is currently unsuited for repeated observations in rodents.

Applications of IVM for Lung Injury Models

With these advanced fluorescence microscopy methods, it is possible to generate high-resolution images of several z-stack positions to generate 3D reconstitutions. The methods described also allow for imaging over several hours to generate time-lapsed data. It is then possible to analyze, localize, and quantify different parameters in four dimensions (3D plus time) such as cell velocity, colocalization, shape, volume, number, intensity, and color. Fluorescence is defined as the emission of light from a fluorescent probe after its excitation by an external light source of defined wavelength. The visualization of tissues, cells or proteins can be

achieved by tagging molecules with specific fluorophores which can be selectively excited and specifically visualized. Here, we describe some useful applications for lung injury models.

- ***Lung morphology and structural changes***

Visualizing the live lung enables the real-time observation of structural changes occurring during injury. For example, changes in lung vessel diameter by intravital microscopy was monitored during sepsis in rats [32] or after hypoxia in mice [26]. To visualize the lung structure several tools are available. Good resolution of the lung matrix can be obtained without using any extrinsic dyes due to the **second harmonic generation** effect. In a tissue, the specific molecular structure of collagen fibers generates an ultraviolet second harmonic light when excited with an infrared laser of a two-photon microscope. **Reporter mice ubiquitously expressing fluorescent proteins** also enable the imaging of stromal cells like the ubiquitously expressed actin-CFP reporter mice [29] or the mTmG reporter mice. A tdTomato fluorophore is expressed ubiquitously in the mTmG mice, and the localization of the fluorescent proteins to membrane structures outlines cell morphology and allows resolution of fine cellular processes (mT). This mouse can be crossed with a Cre-recombinase reporter mouse to target GFP expression in specific cell types (mG). Since the alveoli are surrounded by a dense meshwork of capillaries, **labeling of the blood circulation** by intravascular injection of tagged albumin, polysaccharides (dextran) or untargeted quantum-dots [33] will also produce an excellent outline of the alveolar structure.

- ***Lung edema and vascular leakage***

Lung edema and vascular leakage is a characteristic feature of lung injury. Labeled albumin or labeled polysaccharides (dextran) injected intravenously can also be used to monitor vascular leakage in vivo. Indeed, under homeostatic conditions blood vessels limit the passage of dextran larger than 70 kDa, but during inflammatory conditions, dextran up to 2000 kDa can leak from the intravascular compartment [34]. Dextran efflux and vascular permeability can be quantified by measuring the changes in fluorescent intensity (Fig. 8.2a). The sensitivity of the fluorophore leakage can be modulated by using molecules of different sizes. Fingar et al. used a rat model of lung injury induced by oleic acid or compound 48/80 to directly measure in vivo the kinetics and magnitude of pulmonary vessel leakage and the development of edema. Leakage of intravascular FITC-albumin or rhodamine dye can be observed and quantified [23]. This same method was used to measure FITC dextran leakage after PMA or cigarette smoke-induced lung inflammation [31]. Looney et al. measured in mice the dynamic leakage of Texas Red dextran into the extravascular compartment during lung injury after intratracheal administration of LPS. Interestingly, in vivo imaging revealed a differential rate of vascular leakage across the imaged alveoli [24], an observation that could not have been made using measurement of global lung vascular permeability.

- ***Leukocyte recruitment***

Another typical feature of lung injury is the rapid and massive recruitment of neutrophils into the lungs. Intravital microscopy is one of the most powerful techniques to study the anatomical location and dynamic influx of immune cells, and it is especially valuable for observing trafficking of cells from the circulation to peripheral tissues. Neutrophil recruitment into the lung is different from other vascular beds, and intravital microscopic approaches allow dissecting of these mechanisms in detail. Indeed, the size of a neutrophil (6–8 μm in diameter) can be bigger than the diameter of 50 % of the lung capillaries (2–15 μm). This may explain why neutrophils are sequestered in the lung. Sequestration of neutrophils has been observed in live rabbits by Kuebler et al. [35], and labeled leukocytes confirmed that lung capillaries are the predominant site of leukocyte sequestration. Neutrophil sequestration is accompanied by a morphological change into elongated shapes that have been observed in lung slices by actin labeling and confocal microscopy [36]. The same group made important discoveries about the requirement of selectins in sequestration and emigration of neutrophils in the lung [37]. Different tools are available to study neutrophils in vivo. Cells can be **isolated and fluorescently labeled with vital dyes** before infusion into recipient animals for fluorescence microscopy. Such a method was used by Presson et al. to observe the migration of Rhodamine-6G in vivo-labeled leukocytes into the rat lungs after PMA or cigarette smoke exposure [31]. The same group also demonstrated in a mouse IVM model the role of nitric oxide in neutrophil lung infiltration during sepsis using iNOS knockout mice [38]. Alternatively, the **injection of antibodies tagged** with a range of fluorescent dyes allows for labeling of neutrophils. However, caution must be taken when using this technique as antibodies can induce the activation or the depletion of the targeted cells. Anti-Gr-1, for example, can deplete neutrophils if high doses are used. In addition, the use of **transgenic mice expressing fluorescent proteins in a specific cell lineage** is a powerful method for specific labeling of leukocytes (Fig. 8.2c). A variety of strains have been created to track neutrophils. One example is the lysozyme-M (LysM)-green fluorescent protein (GFP) mouse that is characterized by bright green neutrophils and monocytes that are dim green. Using LysM-GFP mice, Kreisel et al. [27] observed by two-photon intravital imaging the mechanisms of neutrophil extravasation in bacterial pneumonia and ischemia-reperfusion after murine lung transplantation. A large pool of resident lung neutrophils was observed that rapidly increased in number after inflammatory challenge. Neutrophils clustered around monocytes, and the depletion of monocytes reduced this clustering phenomenon and reduced neutrophil extravasation. In the same mouse model of ischemia-reperfusion injury. They established that alveolar macrophages and their cell membrane associated protein DAP12 were important for the production of the chemokine CXCL2 and subsequent neutrophil extravasation [33]. However, LysM is expressed in the lung by both neutrophils and macrophages. To obtain fluorescent expression that is more restricted to neutrophils, the MRP8 promoter has been used [39]. Table 8.1 describes mouse strains commonly used to visualize cells in lung injury models.

Table 8.1 Fluorescent transgenic mice commonly used for lung injury models

Promoter/name	Reporter	Target cells
Lysozyme-M	GFP	Neutrophils, monocytes, macrophages
MRP8	GFP	Neutrophils
CX3CR1	GFP	Monocytes (low), macrophages (high), DC (int)
c-fms	YFP, GFP	Neutrophils, macrophages
CD11c	YFP	Dendritic cells, macrophages
PF4	tdTomato	Platelets
CD41	YFP	Platelets
Tie2	GFP	Blood vessels
Prox1	GFP	Lymphatic vessels
Actin	CFP	Ubiquitous
mTmG	tdTomato	Ubiquitous (membrane)
Lyn	Venus, GFP	Ubiquitous (membrane)

- ***Dynamic cell-cell interactions***

The spatiotemporal observation of cell–cell interactions can stimulate new hypotheses about functional communications between cells and improve the understanding of lung inflammation. In a mouse model of lung injury after lung transplantation, Kreisel et al. [40] used CD11c-eYFP donor lungs transplanted into LysM-GFP recipient mice to observe direct interactions between donor dendritic cells and recipient neutrophils. These studies led to the discovery of a previously unknown link between neutrophils and DCs after lung transplantation that can explain the early events in lung inflammation. After *B. anthracis* pulmonary infection, the agent of anthrax, researchers also observed by IVM the interaction between DCs and alveolar macrophages using CX3CR1-GFP mice [30].

- ***Protein staining and cellular functions***

Monitoring the expression of an important protein is also possible. Fingar et al. used the lung intravital method in rats to determine when and where in the pulmonary vasculature the adhesion molecule ICAM-1 was expressed after TNF-α-induced inflammation [28]. To be able to detect ICAM-1 binding sites under IVM, a two-step labeling procedure was used involving a monoclonal antibody against ICAM conjugated with fluorescent beads that generate enough fluorescence for detection. In addition, mice carrying reporters for cytokines such as IL-4 and interferon-γ have been made and can be used to image functional responses and cell fate decisions in real time.

- ***Platelet biology***

The role of platelets during lung inflammation and injury has received increased attention in recent studies. The interaction of activated platelets with endothelium and neutrophils is important in influencing neutrophil sequestration and activation during the initial phases of lung injury. Lung intravital microscopy is an appropriate

method to investigate the dynamics and mechanisms of these heterotypic interactions. Methods to label platelets include using transgenic animals (CD41-YFP, PF4-tdTomato) and fluorescent monoclonal antibodies (CD49b, CD42b). Intravital microscopy studies in rabbit [41] and mouse [26] showed the retention of labeled platelets in the lung microcirculation after their activation. Using mice obtained by crossing PF4-tdTomato with LysM-GFP mice, our group was able to visualize by 2-photon IVM the real-time interactions between neutrophils and platelets in LPS-induced lung injury. Neutrophil-platelet aggregates in the lung circulation were observed under homeostatic conditions and their number greatly increased after LPS challenge, including in the alveolar spaces, and could be reduced after aspirin treatment, concomitantly with lung injury reduction [42].

- ***Protease activity (fluorescent substrates)***

Inflammatory proteases, such as neutrophil elastase, have been implicated in the pathophysiology of acute lung injury. Specific protease substrates can be used as activatable reporter probes to localize and quantify protease activity in real time. Cleavage of the probe leads to the liberation of the fluorophore. Elastase [43], MMP [44] and Cathepsin [45]-sensitive probes can be used for a better understanding of protease activity during lung inflammation (Fig. 8.2b).

- ***Cell death, injury, and extracellular DNA***

Lung injury is accompanied by endothelial and epithelial cell death. It can be monitored by the use of cell membrane-impermeable cyanine nucleic acid dyes, which only stain dead cells. Neutrophil activation has been involved in cell injury, but the role of cytotoxic proteases in this cell toxicity is still not clear. Recently, neutrophils have been shown to release in the extracellular space their DNA, covered with neutrophil proteases. These neutrophil extracellular traps (NETs) are believed to serve as an antibacterial defense mechanism. However, data suggest that NETs can, in the delicate lung microcirculation, contribute to lung endothelial injury [46]. NETs, made of characteristic DNA strands, can be stained in vivo with cell impermeable nucleotide dyes [47]. Intravital microscopy could reveal the presence and localization of NETs during lung injury and inform their interaction in situ with leukocytes, platelets, and endothelial/epithelial cells.

Noninvasive Imaging Techniques

Bioluminescence Imaging (BLI)

Principles of Luminescence Imaging

Bioluminescence imaging (BLI) is based on the sensitive detection of visible light produced during a biochemical reaction. The oxidation of the substrate luciferin, in presence of ATP, is catalyzed by the expression of the enzyme luciferase, leading to

the emission of light at 560 nm. The luciferase enzyme is naturally found in the firefly, but can be artificially incorporated into cells and animal models under the control of specific promoters. Light from the cells that express the luciferase reporter gene can then be detected when the appropriate substrate is added. The IVIS imaging system consists of a CCD camera mounted on top of a light impermeable chamber where the animal is placed. A heating stage and anesthetics keep the animal warm and sedated. This imaging modality has proven to be a very powerful methodology to detect luciferase reporter activity in intact animal models.

Advantages and Disadvantages of BLI

BLI is low-cost, noninvasive, and facilitates real-time analysis of lung injury processes at the molecular level in living organisms. Since it is noninvasive, each animal can be imaged at multiple time points. BLI allows acquisition of the whole mouse lung, since it is possible to image as deep as several centimeters within tissue. However, compared to fluorescent methods, the resolution is lower and inflammation can only be localized to the organ level. The sensitivity of the NF-κB luciferase reporter mouse has been questioned in the study of lung inflammation by Hadina et al. [48]. It was demonstrated that low-dose LPS was not able to induce any detectable bioluminescence and was therefore less sensitive than measuring neutrophils or cytokines in lung lavage. A significant and quantifiable signal was detectable in the lungs after an intranasal LPS dose of 1.2 mg/kg. Also, quantitative analysis must be approached with caution since light emission depends on the activity of the promoter gene of interest and on the presence of ATP, oxygen and the substrate. The intensity of light is also dependent on the depth of the labeled cells, since light has to travel through the tissue.

Application of BLI in Lung Injury Models

Bioluminescence provides a noninvasive method to monitor gene expression in vivo. Depending on the targeted gene, BLI can serve different purposes.

- ***NF-κB/luciferase reporter mice***

One of the most extensively used luminescent reporter animals is a transgenic mouse expressing the firefly luciferase under the control of a NF-κB-dependent promoter. These mice enable a quantitative method for evaluating the localization, the timing, and the level of NF-κB activation in vivo during inflammatory models. These mice have been used in lung injury models induced by LPS, *Pseudomonas aeruginosa* [49], TNF-alpha or IL-1beta [50]. This strain is also useful to test if specific interventions or anti-inflammatory therapies [51, 52] can affect the inflammation that is dependent on NF-κB activity. In the lung, Sadikot et al. showed that the host response to *P. aeruginosa* can be altered in the lung epithelium in vivo using adenoviral vectors to activate or inhibit NF-κB [53].

- ***ROS generation and MPO activity by luminol or lucigerin substrate***

Another bioluminescent chemical reaction used is the oxidation of luminol or lucigenin substrate catalyzed by the presence of reactive oxygen species (ROS). ROS play an important role in lung injury, and delineating in real time their generation and contribution can be done using luminescent substrates without the use of transgenic mice. In a lung inflammation model induced by intratracheal zymosan, Han et al. [54] demonstrated increased ROS levels in WT but not in $p47^{phox-/-}$ mice, indicating that NADPH oxidase is the major source of ROS generation. Luminol and lucigenin bioluminescent reactions depend on different ROS species. Neutrophil MPO is involved in luminol conversion and can be used to image acute inflammation and neutrophil enriched areas. Lucigenin bioluminescence can be used to detect NADPH activity from macrophages [55].

- ***Inflammatory cell migration and bacterial load***

The introduction of a luciferase reporter gene into T cells [56], macrophages [57], or other immune cells can be used to follow the trafficking of these cells in lung inflammation and injury models. It can be useful in infectious models of lung injury to monitor the bacterial load in the lung or the circulation. This can be achieved by tracking bioluminescent strains of bacteria (*P. aeruginosa* [49], *S. pneumoniae* [58], *S. aureus* [59], *H. influenza* [60]).

Magnetic Resonance Imaging (MRI)

Principles of MRI

Magnetic Resonance Imaging (MRI) is a noninvasive imaging technique that uses a strong magnetic field and radio waves to excite protons contained in different tissues. When the excited protons realign, they emit a radio frequency absorbed by a receiving coil that allows generation of an image of the tissue.

Advantages and Disadvantages of MRI

One of the biggest advantages of this imaging technique is the absence of ionizing radiation, allowing repeated measurements without risking injury to the lungs. In general, however, lung imaging presents two major problems to the use of magnetic resonance image techniques. Motion induced by respiration is the first problem, which can be improved by synchronized ventilation. The second problem is the reduced discriminating capacity of the air-tissue interface due to high water and air content in lungs, leading to a reduced signal. To improve the resolution, the classical proton MRI has been improved by the addition of ultra-short eco time, which has not only increased the resolution but also reduced the imaging time [61, 62].

The use of hyperpolarized ^{129}Xe and most recently, ^{3}He gas has also drastically increased MRI capability to study structural and functional characteristics of the lungs [63, 64]. The use of contrast agents has propelled MRI imaging to a new level of functionality. Ogasawara et al. showed in a radiation-induced lung injury model in dogs that the addition of a contrast agent (gadolinium-DTPA) allowed the discernment of different radiation pneumonitis phases [65].

Applications of MRI in Lung Injury Models

Experimental acute lung injury revealed that inflammation areas localized by MRI correlated with histological and pathological analyses in an IL1β + TNFα instillation model [66]. High-resolution MRI was used by Bosmann et al. to show the effect of extracellular histones in three different ALI models. Histone presence correlated with lung injury observed in the MR images [67]. MRI was more sensitive than high-resolution computed tomography (HR-CT) for the detection of early pathologic changes induced by hyperoxia [68].

Radiation-Based Imaging Techniques: Micro-CT

Principles of Micro-CT

Micro-Computerized Tomography (CT) imaging utilizes X-rays to form virtual slices that are transformed in 2D or 3D images by the software. The signal that is measured in Hounsfield units (HU) depends on the decay of the x-rays when they cross different tissues. The air has a value of −1000 and water a value of 0.

Advantages and Disadvantages of Micro-CT

This noninvasive technique has the inconvenience of the ionizing radiation that may prevent its repeated use in a short period of time. Although Chandra et al. suggested that the radiation used in CT might have an effect on bone loss [69], other studies suggest that the low dose used does not have any cardiopulmonary effect [70]. The main advantage compared to classical x-rays is the serial acquisition of the images allowing a 3D reconstruction that is more informative than a 2D image. CT imaging is also cheaper and faster than MRI. Computer tomography can be used in studies involving metallic implants, which is not possible with MRI. Respiration-gated micro-CT has solved some of the motion problems relevant to live lung imaging. The use of a faster flat-panel volumetric CT has reduced the acquisition time to a few seconds [71].

Applications of Micro-CT in Lung Injury Models

In a dog model of LPS-induced acute lung injury, the use of computed tomography showed vascular leak and edema formation. In this study, the injection of sphingosine 1-phosphate reduced the vascular leak [72]. In an oleic acid-induced lung injury model, pulmonary parenchymal infiltrates were visible using micro-CT [73]. By measuring lung volumes radiographically at end-inspiration and end-expiration, pulmonary compliance can be calculated using computed tomography. Bleomycin challenge reduced lung compliance (measured by CT) in a mouse model [74]. In a similar model of ALI induced by oleic acid, Perchiazzi et al. demonstrated reduced lung compliance in the injured mice [75]. Finally, Fernandez-Bustillo observed using a LPS-induced ALI model that increased IL-1β levels in BAL correlated with an increase in apex-base CT-derived compliance differences [76].

Radiation-Based Imaging Techniques: PET/SPECT

Principles of PET/SPECT

Gamma ray emission imaging techniques are based on the use of small radiolabeled molecules (tracers) that are injected in the body while a gamma camera records the signal they emit. Positron emission tomography (PET) measures 2 gamma photons emitted in 180° angle separation after the positron emitted by the tracer collides against an electron in the tissue. On the other hand, single photon emission computed tomography (SPECT) measures single gamma rays emitted by the tracer.

Advantages and Disadvantages of PET/SPECT

The need of a collimator in SPECT imaging reduces the sensitivity and increases the number of artifacts acquired comparing with PET imaging. But the shorter half-life of the isotopes used in PET (typically Fluorine-18) when compared with the isotopes used in SPECT (Thalium-201 or Technetium-99 m), reduces their availability and increases their price. Both techniques use ionizing radiation, which can be deleterious in sequential acquisitions. PET and SECT imaging can be integrated with high-resolution CT imaging to allow the correlation of functional and metabolic abnormalities with morphological features in the lung [77].

Applications of PET/SPECT in Lung Injury Models

Mintun studied vascular permeability induced by oleic acid in a dog lung injury model and showed that gallium-68 labeled transferrin leaked more into the

extravascular space in challenged than in unchallenged lungs [78]. More recently the tracer used in lung injury models has changed to [^{18}F]-flouro-2-deoxy-D-glucose (18F-FDG). This glucose-derived tracer labeled with Fluorine-18, is the principal tracer used in PET scans to analyze lung injury and it is internalized by the glucose transporter-1. FDG used as leukocyte marker, facilitates the study of neutrophil and macrophage recruitment in the lungs. PET scan studies show that the infiltration peak induced by hydrochloric acid is 24–48 h after instillation [79]. FDG can also be used to determine the activation state of neutrophils measured by their uptake of this tracer. PET/CT with 18F-FDG allows the assessment of both lung aeration and neutrophil inflammation as well as an estimation of the regional fraction of blood. Pouzot et al. used this method to validate the use of regional fraction of blood to assess pulmonary blood flow, using PET in both control animals and animals with ALI [80]. SPECT imaging has been used to study endothelial cell death in a hyperoxia model of ALI [81], and it is useful to analyze the alterations of regional blood flow in saline lavaged lungs [82] or lungs treated with oleic acid [83].

Conclusions and Future Directions

Imaging of live tissues, such as the lung, is being increasingly applied to the study of disease processes, and the importance of combining and confirming data with an imaging technique is becoming more common. More importantly, live imaging also provides the opportunity for relevant observations and discoveries that could not have been done by other ex vivo or static methods. In this chapter, we have described different techniques for imaging the lung, illustrating advantages and limitations of the various methods. The recent adaptation of the intravital microscopy technique to the mouse lung has been a step forward for the field and holds much promise. Combined with two-photon fluorescence microscopy, it is probably the best technique to enable imaging of the lung in real time and its natural environment. As lung intravital microscopy is still limited by imaging depth below the pleural surface, an alternative can be the preparation of lung slices for live imaging. The high-resolution of both techniques supports cellular and molecular-scaled analysis like cell interactions and dynamics. Depending on the level of resolution required for the application, other noninvasive methods can be used for morphological studies (MRI, Micro-CT) or functional studies (Bioluminescence, PET/SPECT). Table 8.2 summarizes the parameters important in choosing an imaging technique for biological application.

We described for each method several applications in the scope of lung injury research. We expect that the increasing availability of transgenic mice and molecular reagent to label cells and their subtypes will bring new applications for animal models. Improvement in lung imaging could also be produced through technical advances in microscopy. Confocal and two-photon microscopy require invasive preparations to access the organ, which is particularly challenging for the

Table 8.2 Lung imaging methods. Overview of the methods used in live lung imaging

		Resolution	Application	Imaging depth	Physiological environment	Invasivity
Fluorescence	Lung slices (LLS)	<1 μm	Molecular scale imaging (cells, protein,…)	100 μm (deep layers of the lung accessible)	Ex vivo	Tissue isolated and sectioned
	Perfused Lung (IPL)	<1 μm	Molecular scale imaging (cells, protein,…)	100 μm	Ex vivo-*whole organ*	Isolated tissue
	Intravital (IVM)	<1 μm	Molecular scale imaging (cells, protein,…)	100 μm	In vivo	Surgery required
Bioluminescence		1 mm	Functional imaging (reporter genes)	Whole body	In vivo	Noninvasive
MRI		100 μm	Lung structure	Whole body	In vivo	Noninvasive
Micro-CT		1 μm	Lung structure	Whole body	In vivo	Noninvasive
PET/SPECT		1 mm	Functional imaging (cell activity)	Whole body	In vivo	Noninvasive

lung. Miniaturization of confocal and two-photon microscopes has been developed and is being optimized [84]. The use of confocal endoscopy has been described in the lung [85, 86] and a miniaturized endoscope with an outer diameter of 0.75 mm can be inserted into the animal through a small keyhole incision or through the main bronchi of the mouse [87]. Such an application could address the idealized lung imaging technique—one that produces high-resolution and non- or minimally-invasive in vivo imaging.

References

1. Young J. Malpighi's "De Pulmonibus". Proceedings of the Royal Society of Medicine. 1929;23(1):1–11 (Epub 1929/11/01).
2. Hall HL. A study of the pulmonary circulation by the trans-illumination method. Am J Physiol. 1925;72:446–57.
3. Wearn JT, Ernestene AC, Bromer AW, Barr JW, German WJ, Zschiesche LJ. The normal behavior of the pulmonary blood vessels with observations on the intermittence of the flow of blood in arterioles and capillaries. Am J Physiol. 1934;109:236–56.
4. Terry RJ. A thoracic window for observation of the lung in a living animal. Science. 1939;90 (2324):43–4 (Epub 1939/07/14).
5. Terry RJ. The presence of water on the respiratory surfaces of the lung. Am J Anat. 1964;115:559–68 (Epub 1964/11/01).
6. De Alva WE, Rainer WG. A method of high speed in vivo pulmonary microcinematography under physiologic conditions. Angiology. 1963;14:160–4 (Epub 1963/04/01).
7. Krahl VE. A method of studying the living lung in the closed thorax, and some preliminary observations. Angiology. 1963;14:149–59 (Epub 1963/04/01).
8. Wagner WW Jr. Pulmonary microcirculatory observations in vivo under physiological conditions. J Appl Physiol. 1969;26(3):375–7 (Epub 1969/03/01).
9. Henjakovic M, Sewald K, Switalla S, Kaiser D, Muller M, Veres TZ, et al. Ex vivo testing of immune responses in precision-cut lung slices. Toxicol Appl Pharmacol. 2008;231(1):68–76 (Epub 2008/05/28).
10. Thornton EE, Krummel MF, Looney MR. Live imaging of the lung. Curr Protoc Cytom. 2012;Chap. 12:Unit12 28.
11. Shlyonsky V, Goolaerts A, Mies F, Naeije R. Electrophysiological characterization of rat type II pneumocytes in situ. Am J Respir Cell Mol Biol. 2008;39(1):36–44 (Epub 2008/02/16).
12. Jacobs ER, Bodiga S, Ali I, Falck AM, Falck JR, Medhora M, et al. Tissue protection and endothelial cell signaling by 20-HETE analogs in intact ex vivo lung slices. Exp Cell Res. 2012;318(16):2143–52 Epub 2012/06/13.
13. Lembrechts R, Brouns I, Schnorbusch K, Pintelon I, Kemp PJ, Timmermans JP, et al. Functional expression of the multimodal extracellular calcium-sensing receptor in pulmonary neuroendocrine cells. J Cell Sci. 2013;126(Pt 19):4490–501 (Epub 2013/07/28).
14. Schnorbusch K, Lembrechts R, Pintelon I, Timmermans JP, Brouns I, Adriaensen D. GABAergic signaling in the pulmonary neuroepithelial body microenvironment: functional imaging in GAD67-GFP mice. Histochem Cell Biol. 2013;140(5):549–66 (Epub 2013/04/10).
15. Helms MN, Jain L, Self JL, Eaton DC. Redox regulation of epithelial sodium channels examined in alveolar type 1 and 2 cells patch-clamped in lung slice tissue. J Biol Chem. 2008;283(33):22875–83 (Epub 2008/06/11).
16. Looney MR, Bhattacharya J. Live imaging of the lung. Annu Rev Physiol. 2014;76:431–45 (Epub 2013/11/20).

17. Chouteau JM, Obiako B, Gorodnya OM, Pastukh VM, Ruchko MV, Wright AJ, et al. Mitochondrial DNA integrity may be a determinant of endothelial barrier properties in oxidant-challenged rat lungs. Am J Physiol Lung Cell Mol Physiol. 2011;301(6):L892–8 (Epub 2011/09/06).
18. Baufreton C, Kirsch M, Loisance DY. Measures to control blood activation during assisted circulation. Ann Thorac Surg. 1998;66:1837–44.
19. Islam MN, Das SR, Emin MT, Wei M, Sun L, Westphalen K, et al. Mitochondrial transfer from bone-marrow-derived stromal cells to pulmonary alveoli protects against acute lung injury. Nat Med. 2012;18(5):759–65 (Epub 2012/04/17).
20. Ichimura H, Parthasarathi K, Quadri S, Issekutz AC, Bhattacharya J. Mechano-oxidative coupling by mitochondria induces proinflammatory responses in lung venular capillaries. J Clin Invest. 2003;111(5):691–9.
21. Kandasamy K, Sahu G, Parthasarathi K. Real-time imaging reveals endothelium-mediated leukocyte retention in LPS-treated lung microvessels. Microvasc Res. 2012;83(3):323–31 Epub 2012/02/22.
22. Al-Mehdi AB, Song C, Tozawa K, Fisher AB. Ca^{2+}- and PI3 kinase-dependent nitric oxide generation in lung endothelial cells in situ with ischemia. J Biol Chem. 2000;275(51):39807–10.
23. Fingar VH, Taber SW, Wieman TJ. A new model for the study of pulmonary microcirculation: determination of pulmonary edema in rats. J Surg Res. 1994;57(3):385–93 Epub 1994/09/01.
24. Looney MR, Thornton EE, Sen D, Lamm WJ, Glenny RW, Krummel MF. Stabilized imaging of immune surveillance in the mouse lung. Nat Methods. 2011;8(1):91–6 Epub 2010/12/15.
25. Kuhnle GE, Leipfinger FH, Goetz AE. Measurement of microhemodynamics in the ventilated rabbit lung by intravital fluorescence microscopy. J Appl Physiol (1985). 1993;74(3):1462–71 (Epub 1993/03/01).
26. Tabuchi A, Mertens M, Kuppe H, Pries AR, Kuebler WM. Intravital microscopy of the murine pulmonary microcirculation. J Appl Physiol (1985). 2008;104(2):338–46 (Epub 2007/11/17).
27. Kreisel D, Nava RG, Li W, Zinselmeyer BH, Wang B, Lai J, et al. In vivo two-photon imaging reveals monocyte-dependent neutrophil extravasation during pulmonary inflammation. Proc Natl Acad Sci USA. 2010;107(42):18073–8 Epub 2010/10/07.
28. Fingar VH, Taber SW, Buschemeyer WC, ten Tije A, Cerrito PB, Tseng M, et al. Constitutive and stimulated expression of ICAM-1 protein on pulmonary endothelial cells in vivo. Microvasc Res. 1997;54(2):135–44 Epub 1997/11/05.
29. Hasegawa A, Hayashi K, Kishimoto H, Yang M, Tofukuji S, Suzuki K, et al. Color-coded real-time cellular imaging of lung T-lymphocyte accumulation and focus formation in a mouse asthma model. J Allergy Clin Immunol. 2010;125(2):461–8 e6 (Epub 2009/12/25).
30. Fiole D, Deman P, Trescos Y, Mayol JF, Mathieu J, Vial JC, et al. Two-photon intravital imaging of lungs during anthrax infection reveals long-lasting macrophage-dendritic cell contacts. Infect Immun. 2014;82(2):864–72 Epub 2014/01/31.
31. Presson RG Jr, Brown MB, Fisher AJ, Sandoval RM, Dunn KW, Lorenz KS, et al. Two-photon imaging within the murine thorax without respiratory and cardiac motion artifact. Am J Pathol. 2011;179(1):75–82 Epub 2011/06/28.
32. McCormack DG, Mehta S, Tyml K, Scott JA, Potter R, Rohan M. Pulmonary microvascular changes during sepsis: evaluation using intravital videomicroscopy. Microvasc Res. 2000;60 (2):131–40 Epub 2000/08/31.
33. Spahn JH, Li W, Bribriesco AC, Liu J, Shen H, Ibricevic A, et al. DAP12 expression in lung macrophages mediates ischemia/reperfusion injury by promoting neutrophil extravasation. J Immunol. 2015;194(8):4039–48 Epub 2015/03/13.
34. Egawa G, Nakamizo S, Natsuaki Y, Doi H, Miyachi Y, Kabashima K. Intravital analysis of vascular permeability in mice using two-photon microscopy. Sci Rep. 2013;3:1932 (Epub 2013/06/05).

35. Kuebler WM, Kuhnle GE, Groh J, Goetz AE. Leukocyte kinetics in pulmonary microcirculation: intravital fluorescence microscopic study. J Appl Physiol (1985). 1994;76(1):65–71 (Epub 1994/01/01).
36. Motosugi H, Graham L, Noblitt TW, Doyle NA, Quinlan WM, Li Y, et al. Changes in neutrophil actin and shape during sequestration induced by complement fragments in rabbits. Am J Pathol. 1996;149(3):963–73 Epub 1996/09/01.
37. Doyle NA, Bhagwan SD, Meek BB, Kutkoski GJ, Steeber DA, Tedder TF, et al. Neutrophil margination, sequestration, and emigration in the lungs of L-selectin-deficient mice. J Clin Investig. 1997;99(3):526–33 Epub 1997/02/01.
38. Razavi HM, le Wang F, Weicker S, Rohan M, Law C, McCormack DG, et al. Pulmonary neutrophil infiltration in murine sepsis: role of inducible nitric oxide synthase. Am J Respir Crit Care Med. 2004;170(3):227–33 Epub 2004/04/03.
39. Passegue E, Wagner EF, Weissman IL. JunB deficiency leads to a myeloproliferative disorder arising from hematopoietic stem cells. Cell. 2004;119(3):431–43 Epub 2004/10/28.
40. Kreisel D, Sugimoto S, Zhu J, Nava R, Li W, Okazaki M, et al. Emergency granulopoiesis promotes neutrophil-dendritic cell encounters that prevent mouse lung allograft acceptance. Blood. 2011;118(23):6172–82 Epub 2011/10/06.
41. Eichhorn ME, Ney L, Massberg S, Goetz AE. Platelet kinetics in the pulmonary microcirculation in vivo assessed by intravital microscopy. J Vasc Res. 2002;39(4):330–9 Epub 2002/08/21.
42. Ortiz-Munoz G, Mallavia B, Bins A, Headley M, Krummel MF, Looney MR. Aspirin-triggered 15-epi-lipoxin A4 regulates neutrophil-platelet aggregation and attenuates acute lung injury in mice. Blood. 2014;124(17):2625–34 (Epub 2014/08/22).
43. Kossodo S, Zhang J, Groves K, Cuneo GJ, Handy E, Morin J, et al. Noninvasive in vivo quantification of neutrophil elastase activity in acute experimental mouse lung injury. Int J Mol Imaging. 2011;2011:581406 Epub 2011/09/24.
44. Bremer C, Tung CH, Weissleder R. In vivo molecular target assessment of matrix metalloproteinase inhibition. Nat Med. 2001;7(6):743–8 Epub 2001/06/01.
45. Haller J, Hyde D, Deliolanis N, de Kleine R, Niedre M, Ntziachristos V. Visualization of pulmonary inflammation using noninvasive fluorescence molecular imaging. J Appl Physiol (1985). 2008;104(3):795–802 (Epub 2008/01/19).
46. Caudrillier A, Kessenbrock K, Gilliss BM, Nguyen JX, Marques MB, Monestier M, et al. Platelets induce neutrophil extracellular traps in transfusion-related acute lung injury. J Clin Invest. 2012;122(7):2661–71.
47. Kolaczkowska E, Jenne CN, Surewaard BG, Thanabalasuriar A, Lee WY, Sanz MJ, et al. Molecular mechanisms of NET formation and degradation revealed by intravital imaging in the liver vasculature. Nat Commun. 2015;6:6673 Epub 2015/03/27.
48. Hadina S, Wohlford-Lenane CL, Thorne PS. Comparison of in vivo bioluminescence imaging and lavage biomarkers to assess pulmonary inflammation. Toxicology. 2012;291(1–3):133–8 Epub 2011/12/03.
49. Sadikot RT, Zeng H, Yull FE, Li B, Cheng DS, Kernodle DS, et al. p47phox deficiency impairs NF-kappa B activation and host defense in Pseudomonas pneumonia. J Immunol. 2004;172(3):1801–8 Epub 2004/01/22.
50. Carlsen H, Moskaug JO, Fromm SH, Blomhoff R. In vivo imaging of NF-kappa B activity. J Immunol. 2002;168(3):1441–6 (Epub 2002/01/22).
51. Sadikot RT, Jansen ED, Blackwell TR, Zoia O, Yull F, Christman JW, et al. High-dose dexamethasone accentuates nuclear factor-kappa b activation in endotoxin-treated mice. Am J Respir Crit Care Med. 2001;164(5):873–8 Epub 2001/09/11.
52. Kim KH, Kwun MJ, Choi JY, Ahn KS, Oh SR, Lee YG, et al. Therapeutic effect of the tuber of alisma orientale on lipopolysaccharide-induced acute lung injury. Evid-Based Complement Altern Med: eCAM. 2013;2013:863892 (Epub 2013/08/29).
53. Sadikot RT, Zeng H, Joo M, Everhart MB, Sherrill TP, Li B, et al. Targeted immunomodulation of the NF-kappaB pathway in airway epithelium impacts host defense against Pseudomonas aeruginosa. J Immunol. 2006;176(8):4923–30 (Epub 2006/04/06).

54. Han W, Li H, Segal BH, Blackwell TS. Bioluminescence imaging of NADPH oxidase activity in different animal models. J Visualized Exp: JoVE. 2012(68) (Epub 2012/11/03).
55. Tseng JC, Kung AL. In vivo imaging of inflammatory phagocytes. Chem Biol. 2012;19 (9):1199–209 Epub 2012/09/25.
56. Dugger KJ, Chrisman T, Jones B, Chastain P, Watson K, Estell K, et al. Moderate aerobic exercise alters migration patterns of antigen specific T helper cells within an asthmatic lung. Brain Behav Immun. 2013;34:67–78 Epub 2013/08/10.
57. Lee HW, Jeon YH, Hwang MH, Kim JE, Park TI, Ha JH, et al. Dual reporter gene imaging for tracking macrophage migration using the human sodium iodide symporter and an enhanced firefly luciferase in a murine inflammation model. Mol Imaging Biol: MIB: Official Publication the Acad Mol Imaging. 2013;15(6):703–12 Epub 2013/05/17.
58. Francis KP, Yu J, Bellinger-Kawahara C, Joh D, Hawkinson MJ, Xiao G, et al. Visualizing pneumococcal infections in the lungs of live mice using bioluminescent Streptococcus pneumoniae transformed with a novel gram-positive lux transposon. Infect Immun. 2001;69 (5):3350–8 Epub 2001/04/09.
59. Francis KP, Joh D, Bellinger-Kawahara C, Hawkinson MJ, Purchio TF, Contag PR. Monitoring bioluminescent Staphylococcus aureus infections in living mice using a novel luxABCDE construct. Infect Immun. 2000;68(6):3594–600 Epub 2000/05/19.
60. Jurcisek JA, Bookwalter JE, Baker BD, Fernandez S, Novotny LA, Munson RS Jr, et al. The PilA protein of non-typeable Haemophilus influenzae plays a role in biofilm formation, adherence to epithelial cells and colonization of the mammalian upper respiratory tract. Mol Microbiol. 2007;65(5):1288–99 (Epub 2007/07/25).
61. Egger C, Cannet C, Gerard C, Jarman E, Jarai G, Feige A, et al. Administration of bleomycin via the oropharyngeal aspiration route leads to sustained lung fibrosis in mice and rats as quantified by UTE-MRI and histology. PLoS One. 2013;8(5):e63432 (Epub 2013/05/15).
62. Wurnig MT, Y; Weiger, M; Jungraithmayr, W; Boss, A. Assessing lung transplantation ischemia-reperfusion injury by microcomputed tomography and ultrashort echo-time magnetic resonance imaging in a mouse model. Invest Radiol. 2013;49(1):23–8.
63. Rudolph A, Markstaller K, Gast KK, David M, Schreiber WG, Eberle B. Visualization of alveolar recruitment in a porcine model of unilateral lung lavage using ^{3}He-MRI. Acta Anaesthesiol Scand. 2009;53(10):1310–6 (Epub 2009/08/18).
64. Thomas AC, Nouls JC, Driehuys B, Voltz JW, Fubara B, Foley J, et al. Ventilation defects observed with hyperpolarized ^{3}He magnetic resonance imaging in a mouse model of acute lung injury. Am J Respir Cell Mol Biol. 2011;44(5):648–54 Epub 2010/07/03.
65. Ogasawara NS, K; Karino, Y; Matsunaga, N. Perfusion characteristics of radiation-injured lung on Gd-DTPA-enhanced dynamic magnetic resonance imaging. Invest Radiol. 2002;37 (8):448–57.
66. Serkova NJ, Van Rheen Z, Tobias M, Pitzer JE, Wilkinson JE, Stringer KA. Utility of magnetic resonance imaging and nuclear magnetic resonance-based metabolomics for quantification of inflammatory lung injury. Am J Physiol Lung Cell Mol Physiol. 2008;295 (1):L152–61 Epub 2008/04/29.
67. Bosmann M, Grailer JJ, Ruemmler R, Russkamp NF, Zetoune FS, Sarma JV, et al. Extracellular histones are essential effectors of C5aR- and C5L2-mediated tissue damage and inflammation in acute lung injury. FASEB J. 2013;27(12):5010–21 Epub 2013/08/29.
68. Yokoyama TT, S.; Nishi, J.; Yamashita, Y.; Ichikado, K.; Gushima, Y.; Ando, M. Hyperoxia-induced acute lung injury using a pig model: coreelation between MR imaging and histolgic results. Radiat Med. 2001;19(3):131–43.
69. Chandra A, Lan S, Zhu J, Lin T, Zhang X, Siclari VA, et al. PTH prevents the adverse effects of focal radiation on bone architecture in young rats. Bone. 2013;55(2):449–57 Epub 2013/03/08.
70. Detombe SAD-B, J.; Petrov, I. E.; Drangova, M. X-ray dose delivered during a longitudinal micro-CT study has no adverse effect on cardiac and pulmonary tissue in C57Bl/6 mice. Acta Radiol. 2013;54(4):435–41.

71. Greschus S, Kiessling F, Lichy MP, Moll J, Mueller MM, Savai R, et al. Potential applications of flat-panel volumetric CT in morphologic, functional small animal imaging. Neoplasia. 2005;7(8):730–40.
72. McVerry BJ, Peng X, Hassoun PM, Sammani S, Simon BA, Garcia JG. Sphingosine 1-phosphate reduces vascular leak in murine and canine models of acute lung injury. Am J Respir Crit Care Med. 2004;170(9):987–93 Epub 2004/07/30.
73. Zhou Z, Kozlowski J, Schuster DP. Physiologic, biochemical, and imaging characterization of acute lung injury in mice. Am J Respir Crit Care Med. 2005;172(3):344–51 Epub 2005/05/17.
74. Shofer S, Badea C, Auerbach S, Schwartz DA, Johnson GA. A micro-computed tomography-based method for the measurement of pulmonary compliance in healthy and bleomycin-exposed mice. Exp Lung Res. 2007;33(3–4):169–83 Epub 2007/06/15.
75. Perchiazzi G, Rylander C, Derosa S, Pellegrini M, Pitagora L, Polieri D, et al. Regional distribution of lung compliance by image analysis of computed tomograms. Respir Physiol Neurobiol. 2014;201:60–70 Epub 2014/07/16.
76. Fernandez-Bustamante A, Easley RB, Fuld M, Mulreany D, Chon D, Lewis JF, et al. Regional pulmonary inflammation in an endotoxemic ovine acute lung injury model. Respir Physiol Neurobiol. 2012;183(2):149–58 Epub 2012/06/26.
77. Cereda M XY, Kadlecek S, Hamedani H, Rajaei J, Clapp J, Rizi R. Hyperpolarized gas diffusion MRI for the study of atelectasis and acute respiratory distress syndrome. 2014.
78. Mintun MD, DR; Welch, MJ; Mathias, CJ; Schuster, DP. Measurements of pulmonary vascular permeability with PETand gallium-68 transferrin. J Nucl Med. 1987;28:1704–16.
79. Zambelli V, Di Grigoli G, Scanziani M, Valtorta S, Amigoni M, Belloli S, et al. Time course of metabolic activity and cellular infiltration in a murine model of acid-induced lung injury. Intensive Care Med. 2012;38(4):694–701 Epub 2012/01/27.
80. Pouzot C, Richard JC, Gros A, Costes N, Lavenne F, Le Bars D, et al. Noninvasive quantitative assessment of pulmonary blood flow with 18F-FDG PET. J Nucl Med. 2013;54 (9):1653–60 Epub 2013/08/03.
81. Audi SH, Jacobs ER, Zhao M, Roerig DL, Haworth ST, Clough AV. In vivo detection of hyperoxia-induced pulmonary endothelial cell death using (99 m)Tc-duramycin. Nucl Med Biol. 2015;42(1):46–52 Epub 2014/09/15.
82. Max MN, B.; Dembinski, R.; Schulz, G.; Kuhlen, R.; Buell, U.; Rossaint, R. Changes in pulmonary blood flow during gaseous and partial liquid ventilation in experimental acute lung injury. Anesthesiology. 2000;96(6):1437–45.
83. Lamm WG, MM; Albert, RK. Mechanism by which the prone position improves oxygenation in acute lung injury. Am J Respir Crit Care Med. 1994;150:184–93.
84. Murugkar S, Smith B, Srivastava P, Moica A, Naji M, Brideau C, et al. Miniaturized multimodal CARS microscope based on MEMS scanning and a single laser source. Opt Express. 2010;18(23):23796–804 Epub 2010/12/18.
85. Chagnon F, Fournier C, Charette PG, Moleski L, Payet MD, Dobbs LG, et al. In vivo intravital endoscopic confocal fluorescence microscopy of normal and acutely injured rat lungs. Lab Invest J Tech Methods Pathol. 2010;90(6):824–34 Epub 2010/04/14.
86. Gu M, Kang H, Li X. Breaking the diffraction-limited resolution barrier in fiber-optical two-photon fluorescence endoscopy by an azimuthally-polarized beam. Sci Rep. 2014;4:3627 Epub 2014/01/11.
87. Dames C, Akyuz L, Reppe K, Tabeling C, Dietert K, Kershaw O, et al. Miniaturized bronchoscopy enables unilateral investigation, application, and sampling in mice. Am J Respir Cell Mol Biol. 2014;51(6):730–7 Epub 2014/06/25.